

# UC Davis

## UC Davis Previously Published Works

### Title

Soluble epoxide hydrolase inhibitor, TPPU, increases regulatory T cells pathway in an arthritis model

### Permalink

<https://escholarship.org/uc/item/90w51225>

### Journal

The FASEB Journal, 34(7)

### ISSN

0892-6638

### Authors

Trindade-da-Silva, Carlos A  
Clemente-Napimoga, Juliana T  
Abdalla, Henrique B  
et al.

### Publication Date

2020-07-01











### DOI

10.1096/fj.202000415r

Peer reviewed

## RESEARCH ARTICLE

# Soluble epoxide hydrolase inhibitor, TPPU, increases regulatory T cells pathway in an arthritis model

Carlos A. Trindade-da-Silva<sup>1</sup>  | Juliana T. Clemente-Napimoga<sup>1</sup>  | Henrique B. Abdalla<sup>1</sup>  | Sergio Marcolino Rosa<sup>1</sup>  | Carlos Ueira-Vieira<sup>2</sup>  | Christophe Morisseau<sup>3</sup>  | Waldiceu A. Verri Jr<sup>4</sup>  | Victor Angelo Martins Montalli<sup>1</sup>  | Bruce D. Hammock<sup>3,5</sup>  | Marcelo H. Napimoga<sup>1</sup> 

<sup>1</sup>Laboratory of Neuroimmune Interface of Pain Research, Faculdade São Leopoldo Mandic, Instituto São Leopoldo Mandic, Campinas, Brazil

<sup>2</sup>Laboratory of Genetics, Institute of Biotechnology, Federal University of Uberlandia, Uberlandia, Brazil

<sup>3</sup>Department of Entomology and Nematology, UC Davis Comprehensive Cancer Center, University of California, Davis, CA, USA

<sup>4</sup>Department of Pathological Sciences, Biological Sciences Center, State University of Londrina – UEL, Londrina, Brazil

<sup>5</sup>EicOsis LLC, Davis, CA, USA

## Correspondence

Marcelo H. Napimoga, Laboratory of Neuroimmune Interface of Pain Research, Faculdade São Leopoldo Mandic, Instituto São Leopoldo Mandic, R. José Rocha Junqueira, 13 Campinas/SP, 13045-755, Brazil.

Email: marcelo.napimoga@gmail.com, marcelo.napimoga@slmandic.edu.br

## Funding information

Fundação de Amparo à Pesquisa do Estado de São Paulo (FAPESP), Grant/Award Number: 2017/22334-9; MCTI | Conselho Nacional de Desenvolvimento Científico e Tecnológico (CNPq), Grant/Award Number: 302527/2019-2; Coordenação de Aperfeiçoamento de Pessoal de Nível Superior (CAPES), Grant/Award Number: 001; HHS | NIH | National Institute of

## Abstract

Epoxyeicosatrienoic acids (EET) and related epoxy fatty acids (EpFA) are endogenous anti-inflammatory compounds, which are converted by the soluble epoxide hydrolase (sEH) to dihydroxyethersatrienoic acids (DHETs) with lessened biological effects. Inhibition of sEH is used as a strategy to increase EET levels leading to lower inflammation. Rheumatoid arthritis is a chronic autoimmune disease that leads to destruction of joint tissues. This pathogenesis involves a complex interplay between the immune system, and environmental factors. Here, we investigate the effects of inhibiting sEH with 1-trifluoromethoxyphenyl-3-(1-propionylpiperidin-4-yl) urea (TPPU) on a collagen-induced arthritis model. The treatment with TPPU ameliorates hyperalgesia, edema, and decreases the expression of important pro-inflammatory cytokines of Th1 and Th17 profiles, while increasing Treg cells. Considering the challenges to control RA, this study provides robust data supporting that inhibition of the sEH is a promising target to treat arthritis.

**Abbreviations:** AA, arachidonic acid; APC, antigen-presenting cell; CD, cluster of differentiation; cDNA, complementary DNA; CFA, complete Freund's adjuvant; CIA, collagen-induced arthritis; CII, collagen type 2; CONCEA, Brazilian National Council for Control of Animal Experimentation; COX, cyclooxygenase; CYP, cytochrome P450; DHETs, dihydroxyeicosatrienoic acids; DMARDs, disease-modifying antirheumatic drugs; EET, epoxyeicosatrienoic acids; EpFA, epoxy fatty acids; FOXP3, forkhead box P3; GAPDH, glyceraldehyde 3-phosphate dehydrogenase; H&E, hematoxylin & Eosin; HO-1, heme oxygenase-1; IFN- $\gamma$ , interferon; IL, interleukin; kg, kilograms; LOX, lipoxigenase; mg, milligrams; mm, millimeters; MTX, methotrexate; Nrf-2, nuclear factor erythroid 2-related factor 2; nM, nanomolar; OPG, osteoprotegerin; PCR, polymerase chain reaction; PEG, poly(ethylene glycol); RA, rheumatoid arthritis; RANKL, receptor activator of nuclear factor kappa-B ligand; ROR- $\gamma$ t, retinoic-acid-receptor-related orphan nuclear receptor gamma; sEH, soluble epoxide hydrolase; Tbet, T-box transcription factor; TBST, tris-buffered saline; TGF- $\beta$ , transforming growth factor beta; TNF- $\alpha$ , tumor necrosis factor alpha; TPPU, 1-trifluoromethoxyphenyl-3-(1-propionylpiperidin-4-yl) urea; Tregs, regulatory T cells;  $\mu$ l, microliter.

This is an open access article under the terms of the Creative Commons Attribution-NonCommercial License, which permits use, distribution and reproduction in any medium, provided the original work is properly cited and is not used for commercial purposes.

© 2020 The Authors. *The FASEB Journal* published by Wiley Periodicals LLC on behalf of Federation of American Societies for Experimental Biology

Environmental Health Sciences (NIEHS),  
Grant/Award Number: R35 ES030443 and  
P42ES04699

**KEYWORDS**

rheumatoid arthritis, soluble epoxide hydrolase, TPPU, Th1, Th17, Treg

## 1 | INTRODUCTION

Rheumatoid arthritis (RA) is a chronic inflammatory disease that assaults joints. Elevated levels of proinflammatory cytokines, such as TNF- $\alpha$ , IL-6, IL-17 and IL-33, contribute to synovial inflammation.<sup>1</sup> Glucocorticoids are widely used to relieve pain and swelling and move to final form consequently control of inflammation. However, chronic use produces unwanted side effects. To control long-term inflammation, disease-modifying antirheumatic drugs (DMARDs) are needed to avoid the use of glucocorticoids.<sup>2</sup> Methotrexate (MTX) is the standard first-line therapy of RA. However, about 40% of RA patients are unresponsive to MTX treatment.<sup>3</sup> Evidence demonstrates that cytokines are successful therapeutic targets in RA, which include anti-TNF- $\alpha$  and anti-IL-1 $\beta$  therapies, however several side effects have been described specially infections.<sup>4,5</sup> To sum up, the literature underscores the need for new therapeutic avenues to treat RA.

Arachidonic acid (AA) is metabolized through several pathways, such as the cyclooxygenase (COX) pathway that yields prostaglandins, and lipoxygenase (LOX) that produces the leukotrienes. These pathways are central to current treatment strategies related to inflammation and pain. However, more recently a third partway has been studied; cytochrome P450s (CYP)-dependent AA derivatives notably gives rise to epoxyeicosatrienoic acids (EET) and other epoxy fatty acids (EpFA), which are effective and important bioactive lipids, controlling pain and inflammation.<sup>6</sup> However, these EETs are converted into 1,2-dihydroxy-fatty acids (DHETs) in the presence of soluble epoxide hydrolase (sEH), losing their ability to control inflammation and sometimes showing proinflammatory effects.<sup>7</sup> Thus, sEH inhibitors were developed in order to increase EET levels in vivo.<sup>8</sup> Recently our group showed that sEH inhibition decreases bone loss by modulating host inflammatory response in an inflammatory bone resorption experimental model, similar to what occurs in arthritis.<sup>9,10</sup> Moreover, in a previous study, using two sEH inhibitors administered per orally to dogs with naturally occurring osteoarthritis, significant reduction of pain was already observed 5 days after treatment initiation compared to placebo, suggesting that altering lipid epoxides could be a therapeutic approach for osteoarthritis.<sup>11</sup> Taken together, these previous results provide a hitherto unrecognized mechanism of immune regulation in RA by sEH inhibitors.

Regulatory T cells (Tregs) are a subset of CD4<sup>+</sup> T cells critical for immune homeostasis, preventing the onset of auto-immunity diseases. Treg cells achieve this immunoregulatory control through multiple suppressive mechanisms that inhibit cells responsible for innate immunity, antigen-presenting cell

(APC) functions, as well as adaptive B, CD4<sup>+</sup> and CD8<sup>+</sup> effector T (Teff) cell responses.<sup>12</sup> Manipulation and modulation of Treg cells represent a potent strategy for therapeutic benefit in many related diseases including RA.<sup>13</sup> Herein, we explore the molecular mechanism of sEH inhibition in a RA model by testing the hypothesis that sEH inhibition limits disease outcomes by interfering with the balance between CD4<sup>+</sup> T cells and Tregs favoring enhancement of Tregs.

## 2 | MATERIALS AND METHODS

### 2.1 | Animals and animals care

This study was performed on male mice DBA/1J weighing 25 to 30 g (n = 6/per group), in a total of 30 animals, and kept in cages (5 per cage) in a temperature-controlled room (23  $\pm$  1°C), 12:12 light cycle, with water and food ad libitum. This in vivo protocol was performed according to the “NC3Rs ARRIVE Guidelines, Animal Research: Reporting of in Vivo Experiments”. All experiments were conducted in accordance with the Committee on Animal Research of Faculdade São Leopoldo Mandic, Brazil (#2019/019), which followed the guidelines by the Brazilian National Council for Control of Animal Experimentation (CONCEA).

### 2.2 | Tested drug

The current study used the sEH inhibitor 1-(1-propanoyl) piperidin-4-yl)-3-[4-(trifluoromethoxy)phenyl]urea (TPPU) which was synthesized in-house, purified and chemically characterized as described earlier.<sup>8</sup> The dose tested was 10 mg/kg administered via oral gavage. This dose was chosen based on previous data in mice showing that this dose results in plasma TPPU concentrations of 1780  $\pm$  400 nM after 48 hours and led to significant shifts in the epoxide/diol ratios of all biological important polyunsaturated fatty acids.<sup>14</sup> In addition, previous data obtained from our group, support the efficacy of the current dose.<sup>9,10</sup>

### 2.3 | Collagen-induced Arthritis (CIA) in DBA/1J mice

CIA was elicited in mice as previously described.<sup>15</sup> Male DBA/1J mice (6-9 weeks) were immunized intradermally at 1.5 cm from the base of the tail with 100  $\mu$ g of chicken sternal

hyaline Collagen type 2 (CII) (Sigma) dissolved in 100  $\mu$ L acetic acid (0.05 mol/L) and mixed with an equal volume of CFA (Difco Laboratories, Detroit, MI, USA). After 21 days, animals were boosted with 100  $\mu$ g CII emulsified in incomplete Freund's adjuvant (Difco). Mice were monitored daily for signs of arthritis as described. Scores were assigned based on erythema, swelling, or loss of function present in each paw on scale of 0-4, giving a maximum score of 16 per mouse (see below for details). When mice reached a score of 1 for clinical arthritis, the animals were randomly assigned to one of the following group: mice were treated with TPPU (10 mg/kg by gavage) or vehicle (the same volume of PEG400 in saline) daily for 15 days. Scoring was conducted in a blinded fashion by an investigator who do not perform the treatment of the animals. At the end of 15 days, all groups were anesthetized with xylazine and ketamine i.p. and sacrificed by cervical dislocation. Knee and paw joints were collected for histological studies, western blot and quantitative PCR.

## 2.4 | Clinical scores

Mice were inspected for the development of CIA and inflammation of the four paws was graded between 0 and 4:0, paws with no swelling; 1, paws with swelling of finger joints or focal redness; 2, paws with mild swelling of wrist or ankle joints; 3, paws with severe swelling of the entire paw; and 4, paws with deformity or ankylosis. Each paw was graded, and the four scores were added.<sup>16</sup>

Articular edema of paw was assessed through measurements of the transverse diameters using a digital caliper. Thickness values of paw joint were expressed in millimeters (mm).

## 2.5 | Mechanical hyperalgesia

Hyperalgesia tests were evaluated using a von Frey assay.<sup>17</sup> The assessment of nociception in the tibia-tarsal joint consists of the application, through meshes of increasing pressure on the paw of the mouse, until the animal flexes the femur, tibia, producing a paw withdrawal response. The intensity of mechanical hyperalgesia in the joint was measured by the absolute values of the mechanical threshold (in grams).

## 2.6 | Histological analysis

Whole joints were removed on the 15th day after treatment with TPPU, the joints were fixed in 10% neutral-buffered formalin, for 2 days before decalcification in NaOH/EDTA solution (pH 7.4) and processed for paraffin embedding. Tissue longitudinal sections (5  $\mu$ m) were prepared and stained with

H&E. H&E stained femuro-tibial joint sections were examined blinded and scored using light microscopy, and the degree of vascular proliferation and inflammatory infiltrate was determined. The degree of vascular proliferation was classified on a scale of 0-3 (0: normal, 1: mild, 2: moderate, 3: severe) and expressed as the mean of 6 samples accordingly to the groups. The degree of inflammatory infiltrate was evaluated in the same 6 samples and classified on a scale of 0-3 [no inflammation: 0 (absence of inflammatory cells); mild inflammation: 1; moderate inflammation: 2; severe inflammation: 3. The final score was determined by adding the scores above for each of the samples.<sup>18</sup>

Another section was stained by Toudine blue (Sigma) and the areas of femoral and tibial cartilages were measured using ImageJ software.<sup>19</sup> In addition, Masson's Trichrome Stain was used to show collagen and bone, blue marked, in the joint sections.

## 2.7 | Immunohistochemistry

The following primary antibodies were used: anti-FoxP3 (IgG, Gene ID 50943, dilution 1/50), from Novus Biologicals, USA and anti-ROR $\gamma$ t (IgG1, clone 4F3-3C8-2B7, 1/50), from BioLegend, USA. Briefly, the immunohistochemical staining was performed as follows: the 3- $\mu$ m sections were deparaffinized, hydrated and endogenous peroxidase activity was quenched by immersion of the slides in 3% hydrogen peroxide during 3 minutes. The antigen retrieval (AR) was achieved by boiling, in a steamer, in citrate buffer (pH: 6.0) or Tris-EDTA buffer (pH: 8.9) according to the primary antibody used. After cooling, the sections were incubated at 4°C with the primary antibody overnight and then with the Advanced polymer for 1 hour at 37°C. Subsequently, sections were stained for 10 minutes at 37°C with 3,30-diaminobenzidine tetrahydrochloride (DAB) and counter-stained with hematoxylin. Images from each region of interest were obtained using an optical microscope using a 40 and 100 $\times$  objectives.

## 2.8 | Real-time PCRs

The mRNA levels corresponding to RANKL, OPG, IL-12p40, Tbet, IFN- $\gamma$ , ROR- $\gamma$ t IL-17, IL-23, FOXP3, TGF- $\beta$ , IL-10, TNF- $\alpha$ , IL-33, IL-1 $\beta$ , IL-6, HO-1, Nrf-2 and GAPDH were assessed using Real Time PCR. The primer sequences are presented in Table S1. Total RNA was isolated by the TRIzol method (Life Technologies, Rockville, MD), according to the manufacturer's recommendation. RNA samples were resuspended in diethylpyrocarbonate-treated water and stored at -70°C. Reverse transcription total RNA was DNase treated (Turbo DNA-frees; Ambion), and 1  $\mu$ g

was used for cDNA synthesis (cDNA synthesis kit, Roche Diagnostic, Indianapolis, IN), following the manufacturer's recommendations. Primers were designed using a probing design system (Light-Cycler Roche probe design software). Quantitative real-time PCR was performed with FastStart DNA Master PLUS SYBR Green (Roche Diagnostics), using a LightCycler System (Roche Diagnostics). The reaction product was quantified with the Relative Quantification tool, using GAPDH as the reference gene. Negative controls with SYBR Green PCR Master Mix and water were performed for all reactions. Relative gene expression was quantified using the  $\Delta$ CT method and normalized to GAPDH. Negative controls with SYBR Green PCR Master Mix and water were used for all reactions.

## 2.9 | Western blotting

Equal amounts of protein (60  $\mu$ g) from the knee joint tissue were separated by 10% SDS-PAGE, and transferred to a nitrocellulose membrane (Bio-Rad Laboratories, Hercules, CA). A molecular mass standard (Bio-Rad Laboratories) was run in parallel to estimate molecular mass. Membranes were blocked overnight at 4°C in TBST (20 mM Tris-HCl [pH 7.5], 500 mM NaCl, and 0.1% Tween 20) containing 5% of nonfat dried milk. After blocking, the membranes were incubated at 4°C overnight, with anti-sEH (1:1000; Dr Hammock, University of California, Davis) or GAPDH (Santa Cruz Biotechnology, Santa Cruz, CA), used as an internal control (1:1000), diluted in TBST containing 5% of nonfat dried milk, for the analyses of the joint proteins. The membranes were then incubated with appropriate secondary antibody conjugated with peroxidase (1:5000) diluted in TBST containing 5% of nonfat dried milk at room temperature for 60 minutes. Finally, the bands recognized by the specific Ab were visualized using a chemiluminescence-based ECL system (Amersham Biosciences, Piscataway, NJ). Pixel intensities of immunoreactive bands were quantitated using FluorChem Q Imaging software (Alpha Innotech, CA). protein expression was normalized to GAPDH. A computer-based imaging system (ImageJ; National Institutes of Health, Bethesda, MD) was used to measure the OD of the bands.

## 2.10 | Statistical analysis

The statistical analyses were performed using Prism 6.0 (GraphPad, La Jolla, CA, USA). The data were first examined for normality using the Kolmogorov-Smirnov test. Comparison between groups at all times when the parameters were measured at different time points after the stimulus injection was performed using two-way ANOVA. For single time-point, we used one-way ANOVA and the post-test of

Tukey or nonparametric test Kruskal Wallis followed by Dunn test for histopathological scores.  $P < .05$  was considered significant. Data are presented as mean  $\pm$  SD.

## 3 | RESULTS

### 3.1 | Effects of sEH inhibition on clinical scores

We investigated the effects of TPPU, a highly selective inhibitor of sEH, on an arthritis experimental model, in DBA/1J mice. The pathological score, including parameters such as paw volume, pain and clinical evaluation, was monitored until the 15th day after the initial development of the disease (Figure 1C). CIA-induced a time-dependent increase clinical score (Figure 1D), number of the affected paw (Figure 1E), articular mechanical hyperalgesia (Figure 1F) and edema (Figure 1G), from 1-15 days after disease onset. Treatment with TPPU (10 mg/kg) statistically ameliorated clinical score on the paw (Figure 1D) from 9th until the 15th day ( $P < .05$ ), and diminished the number of affected paws in comparison to the CIA positive control group (statistically significant beginning from day 9 until the 15th,  $P < .05$ ). In addition, animals treated with TPPU showed decreased pain (Figure 1F) starting on day 6 as compared to CIA-induced animals ( $P < .05$ ), and had lower edema in the paw (Figure 1G), statistically significant from 9 to the 15th day,  $P < .05$ ). These results suggest that a treatment with TPPU starting after disease onset can reduce RA severity.

### 3.2 | TPPU reduces CIA-induced histopathological articular changes and leukocyte influx

Histopathology analysis of the knee joint demonstrated that CIA-induced a significantly higher degree of vascular proliferation and leukocyte infiltration, specially neutrophils (examples indicated by arrows) and pronounced invasive pannus formation compared to the saline group (Figure 2A). Treatment with TPPU at a dose of 10 mg/kg statistically reduced ( $P < .05$ ) the CIA-induced histopathological changes (Figure 2B).

Additionally, the knee joint inflammation contributes to the cartilage erosion identified as a decrease of proteoglycan concentration. Sections of knee joints were stained for toluidine blue and Masson's Trichrome for histopathological evaluation and quantitative analysis of proteoglycan levels (Figure 3C-H). CIA (Figure 3D,G) induced a significant decrease of proteoglycan concentration in the knee joint 15 days after CIA compared to the vehicle (Figure 3C,F), as observed by toluidine blue staining and quantitative analysis of proteoglycan degradation (Figure 3A,B). On the other hand, the treatment with TPPU inhibited CIA-induced proteoglycan



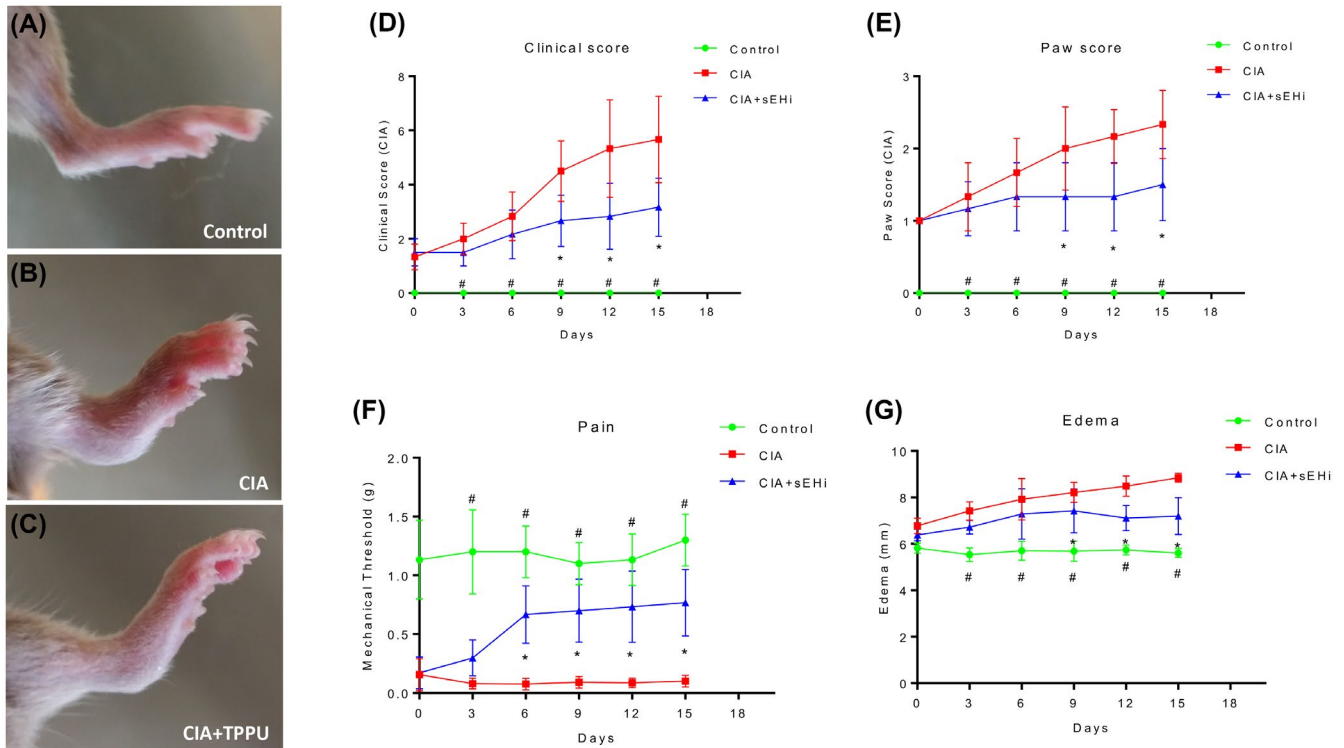


**FIGURE 1** Soluble epoxide hydrolase inhibitor ameliorates CIA score. DBA/1J mice (Naive) or CIA-induced mice were treated daily with vehicle or TPPU (10 mg/kg/animal) for 15 days. Mice were monitored for disease progression (A-C), as indicated by clinical score (D), number of affected paws (E), pain (F) and Edema (G). Results are mean  $\pm$  SD,  $n = 6$  mice per group in each experiment.  $\#P < .05$  vs CIA group;  $*P < .05$  vs CIA group. Two-way ANOVA and post-test of Tukey)

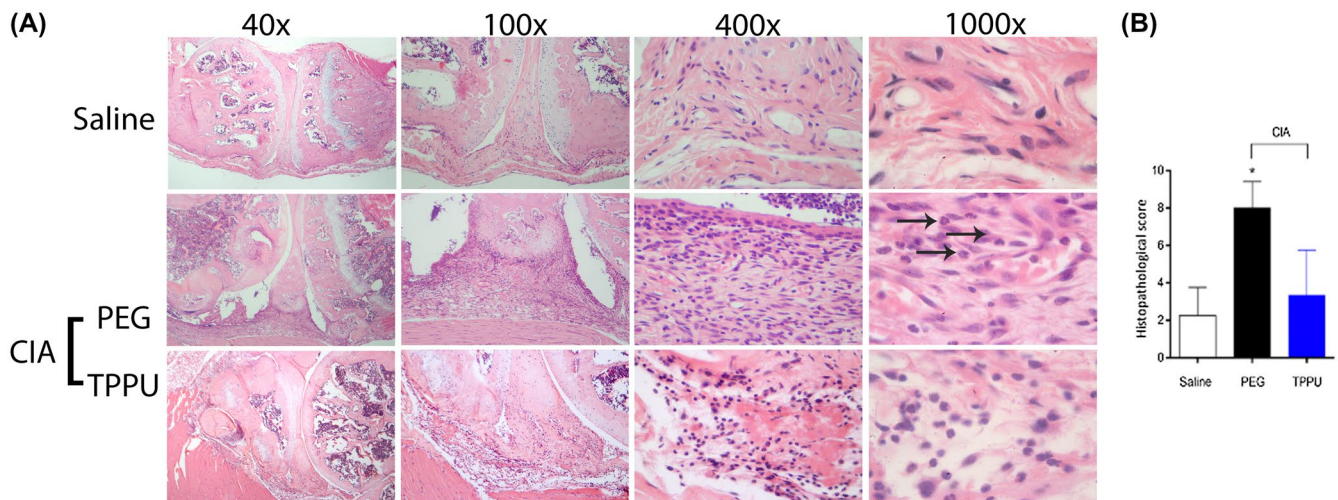


**FIGURE 2** Histopathological score. DBA/1J mice (Saline) or CIA-induced mice were treated orally daily with PEG 400 or TPPU (10 mg/kg/animal) until the 15th day. Histopathological analysis and score were performed in samples of the knee joint collected on day 15. The knee joint sections were stained with H&E. (Hematoxylin and eosin stained, 40, 100, 400 and 1000 $\times$  magnification). Morphological features, showing the inflammatory infiltrate around the bone defects. In the naïve group note few immune cells within stroma; CIA-induced group note immune cells within the stroma of the inflamed and forming an aggregate in the space around the articulation. High neutrophils influx is observed (arrows); TPPU-treated group note immune cells within the stroma. The parameters analyzed were invasive pannus formation; vascular proliferation; and leukocyte infiltration.  $n = 6$ . Results are presented as mean  $\pm$  SD \*indicates statistically significant difference between groups (Kruskal-Wallis followed by Dunn's post hoc test)

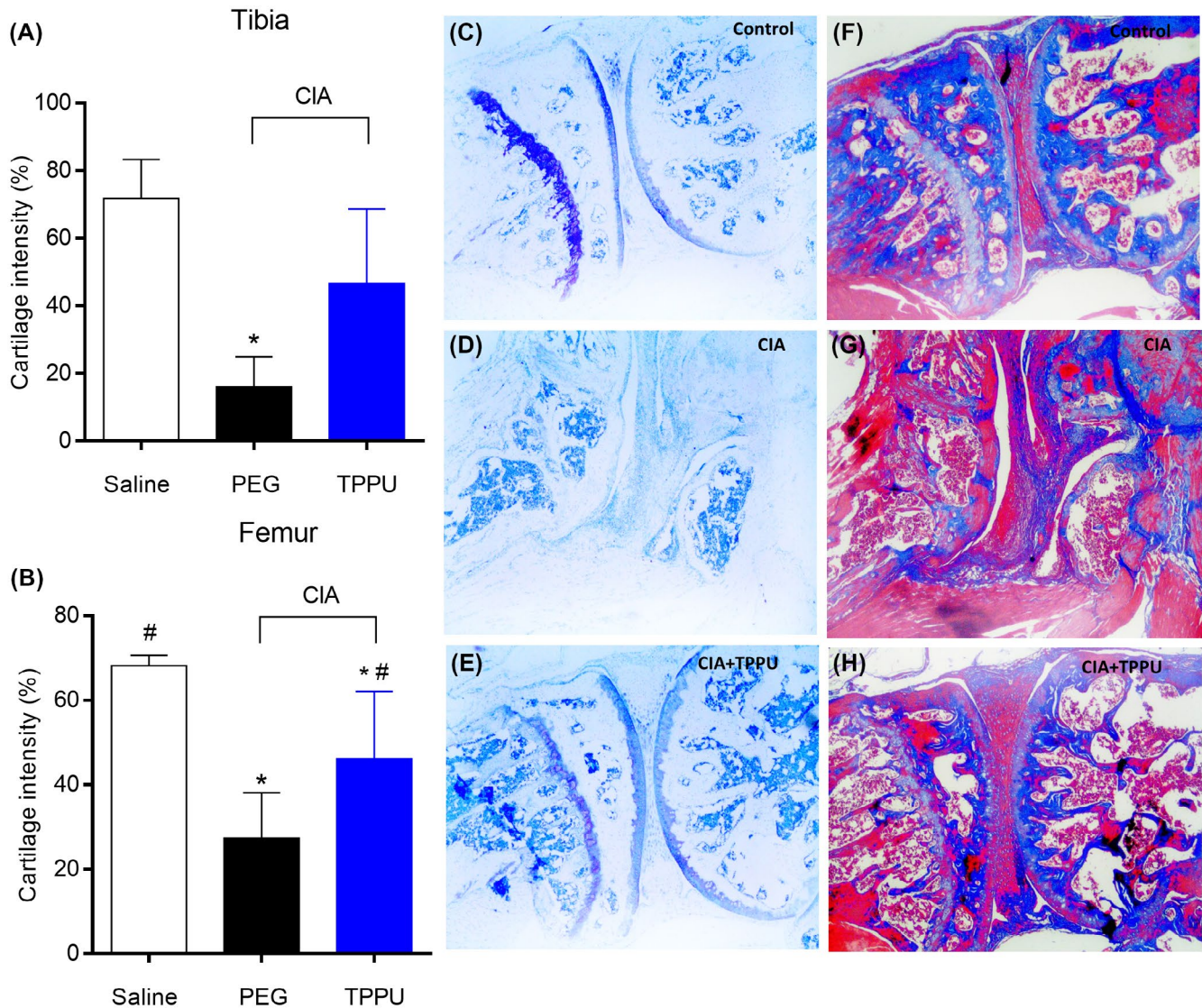


**FIGURE 3** TPPU inhibits proteoglycan degradation. Mice were treated orally with TPPU 10 mg/kg or vehicle (PEG400) for 15 days. Toluidine blue staining; (C-E) quantification of femoral (right side) and tibial (left side) stained areas and Trichrome stain (F-H); A, B, Graphical representation of percentage of stained proteoglycan femoral and tibial areas; Original magnification 40 $\times$ , n = 6. Results are presented as mean  $\pm$  SD. Different symbols indicate statistical significance  $P < .05$  (Kruskal-Wallis followed by Dunn's post hoc test)

loss (Figure 3E,H). The quantitative analysis of proteoglycan degradation from tibial and femur cartilage of the CIA-induced group showed statistical decreased expression (Figure 3A,B;  $P < .05$ ) in comparison to naïve group. The TPPU-treated group statistically protected the proteoglycan degradation at the tibial cartilage (Figure 3A;  $P < .05$ ) and femur cartilage showed a tendency to inhibit the proteoglycan degradation (Figure 3B;  $P = .0615$ ).

### 3.3 | TPPU decreases the sEH expression in the knee joint

The sEH expression has been shown to increase in several diseases<sup>9,20-22</sup> and appear to be a common marker at tissue

inflammation. This is in agreement with our finding that sEH expression was also increased in CIA. Interestingly, in addition to inhibiting sEH function,<sup>8,23</sup> TPPU also decreased sEH protein levels ( $P < .05$ ) (Figure 4). Non-immunized animals had the same level of sEH expression as TPPU-treated animals ( $P > .05$ ), suggesting that sEH could be a target for arthritis treatment.

### 3.4 | TPPU modulates expression of osteoclastogenesis-related proteins (RANKL and OPG) in the knee joint

As observed in Figure 5, levels of RANKL (Figure 5A) were upregulated in CIA animals, compared with non-immunized



animals ( $P < .05$ ). The administration of TPPU (10 mg/kg) statistically reduced the expression of this osteoclastogenesis-related cytokine in animals with arthritis. Also, OPG

expression (Figure 5B) was slightly increased in CIA animals although there is no statistical difference among groups ( $P > .05$ ). Overall, the balance between RANKL and OPG expression is essential to determine the biological response in RA. In the analysis of the RANKL/OPG ratio, CIA animals showed statistically elevated expression in comparison to control animals and TPPU-treated animals (Figure 5C,  $P < .05$ ).

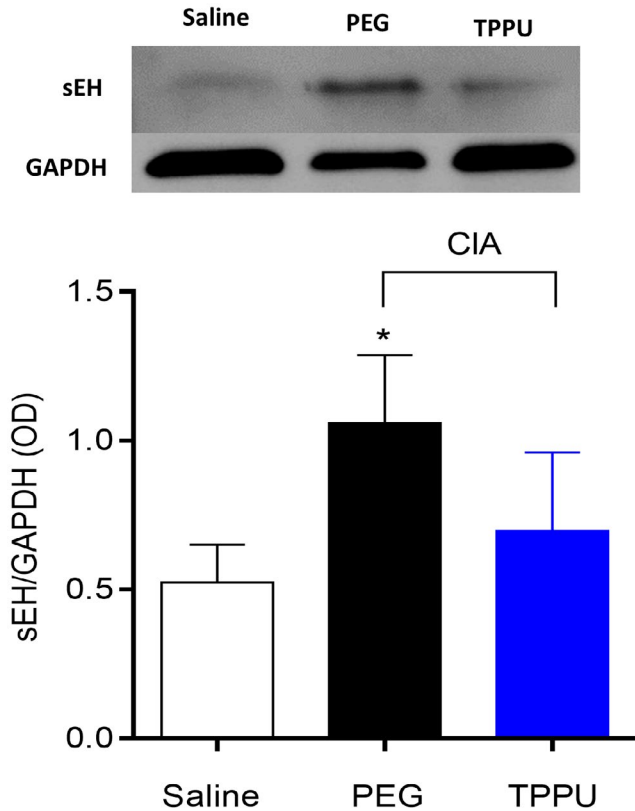


**FIGURE 4** Expression of soluble epoxide hydrolase (sEH) protein in the knee joint. Protein expression of sEH in joint tissues (soft tissue, fluid and bone) of all experimental groups analyzed by Western blotting. Density of the sEH bands was normalized to that of GAPDH. Protein band intensity is represented as arbitrary units (mean  $\pm$  SD) ( $n = 6$ ). \*indicates statistical significant difference between groups (one-way ANOVA followed by Tukey test)

### 3.5 | Effects of sEH inhibition on patterns of cytokine expression in arthritis

Th1 cells differentiate in the presence of IL-12, and require activation of the master regulator transcription factor, T-bet, that induces IFN- $\gamma$  production<sup>24</sup> CIA animals showed statistically increased expression of genes related to Th1 profile (Figure 6A-C), while TPPU treatment animals abrogated the expression of Th1 cells profile ( $P < .05$ ).

Interleukin-23 (IL-23) plays an important role in expanding and maintaining the Th17 cell population, up-regulating the expression of ROR $\gamma$ t, a specific transcriptional regulator for the expression of interleukin-17.<sup>25</sup> Our results demonstrated that the IL-23, ROR- $\gamma$ t and IL-17 expression, were statistically upregulated in the CIA group ( $P < .05$ ) when compared with non-immunized group (Figure 6D-F). A decrease of IL-23 and IL-17 gene expression was observed in TPPU-treated animals ( $P < .05$ ) with a trend towards a decrease of ROR- $\gamma$ t expression without statistical significance.

The transcription factor Foxp3 is a specific factor which identifies regulatory T cells (Treg). These cells produce anti-inflammatory cytokines like TGF- $\beta$  and IL-10 and also help to maintain immune homeostasis.<sup>26</sup> Interestingly, inhibition of sEH with TPPU statistically increased the Foxp3 and TGF- $\beta$  expression (Figure 6G,H) when compared with

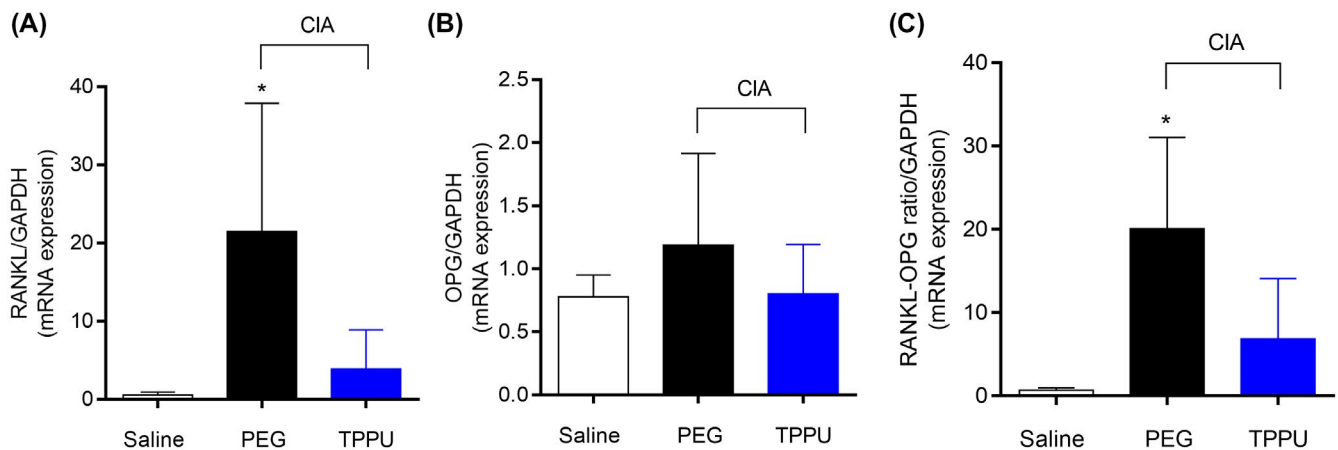


**FIGURE 5** Bone related markers expression. mRNA quantification of RANKL (A), OPG (B) and RANKL/OPG ratio were performed in joints on day 15 of TPPU treatment. Results are presented as mean  $\pm$  SD ( $n = 6$ ). \*indicates statistical significant difference between groups (one-way ANOVA followed by Tukey test)



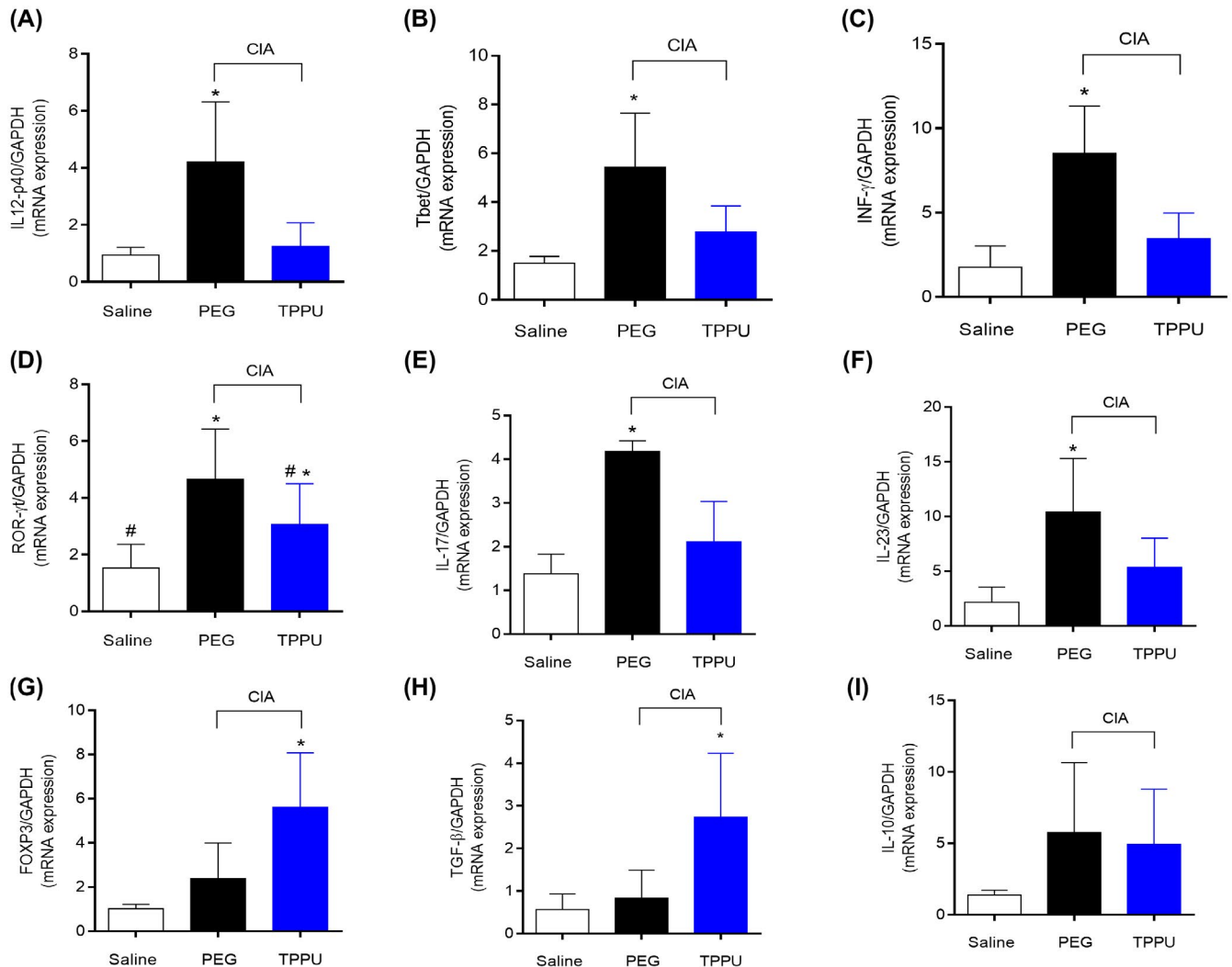


**FIGURE 6** sEHi immunomodulates cytokines and induces polarization of lymphocytes. mRNA quantification to IL-12p40 (A), T-bet (B) IFN- $\gamma$  (C) ROR- $\gamma$ t (D) IL-17 (E) IL-23 (F), FOXP3 (G) TGF- $\beta$  (H) and IL-10 (I) were performed in joints (soft tissue, fluid and bone) on day 15 of TPPU treatment. (n = 6). \*indicates statistical significant difference between groups (one-way ANOVA followed by Tukey test)

CIA-induced animals ( $P < .05$ ). The IL-10 expression was elevated in both groups CIA and TPPU-treated, however there is no statistical difference among the groups (Figure 6I).

To demonstrate the FOXP3+ cells and ROR- $\gamma$ t+ cells in the joint of the animals, it was performed an immunohistochemistry analysis. The naïve group showed no immunoreactive cells while CIA-induced group exhibited numerous positive staining cells for ROR- $\gamma$  when compared to staining for the TPPU-treated group (Figure 7). On the other hand, the TPPU-treated group presented higher FOXP3+ cells than the CIA-induced group (Figure 8), corroborating the qPCR data.

Moreover, the pro-inflammatory cytokines TNF- $\alpha$ , IL-33, IL-6 and IL-1 $\beta$  (Figure 9A-D) were statistically overexpressed in CIA-induced animals ( $P < .05$ ) when compared with the non-immunized group as well as with TPPU-treated animals. The gene expression to Heme Oxygenase 1 (HO-1), is induced by the transcription factor Nrf-2 (nuclear factor erythroid 2-related factor 2). HO-1 is responsible for several

anti-inflammatory effects, decreasing pro-inflammatory cytokines levels.<sup>27</sup> CIA-induced animals showed decreased expression levels of HO-1 (Figure 9E) and Nrf-2 (Figure 9F) although not statistically different when compared to non-immunized animals. However, TPPU-treated animals were able to statistically increase the expression of both markers ( $P < .05$ ).

## 4 | DISCUSSION

Millions of Americans have pain caused by some form of arthritis.<sup>28</sup> Subsequently, pain and disability may occur resulting in a reduced quality of life.<sup>29</sup> RA is a chronic, progressive inflammatory disease of synovial joints. Chronic inflammation results from aberrant innate and adaptive immune responses that contribute to drive RA to the point of joint failure.<sup>30</sup> The current therapy of RA is complex and

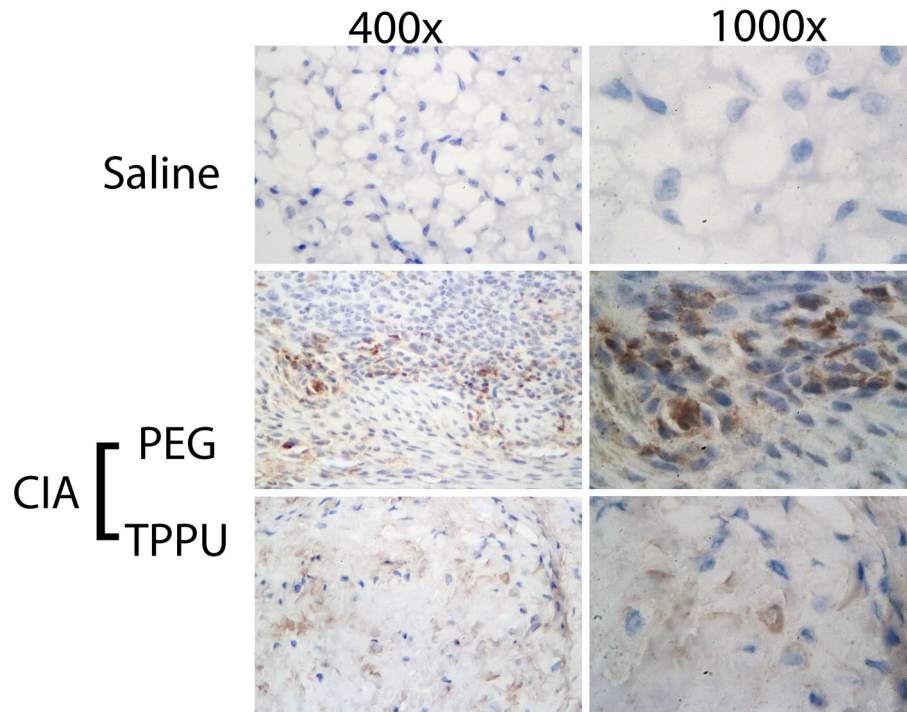


**FIGURE 7** Immunohistochemical staining for ROR- $\gamma$ t. Immunostaining was performed in knee joint. Naïve animals showed no immunostaining staining. CIA-induced exhibited a several positive immunostaining cells and fewer immunostaining cells were observed in the TPPU-treated group (400 and 1000 $\times$  magnification)

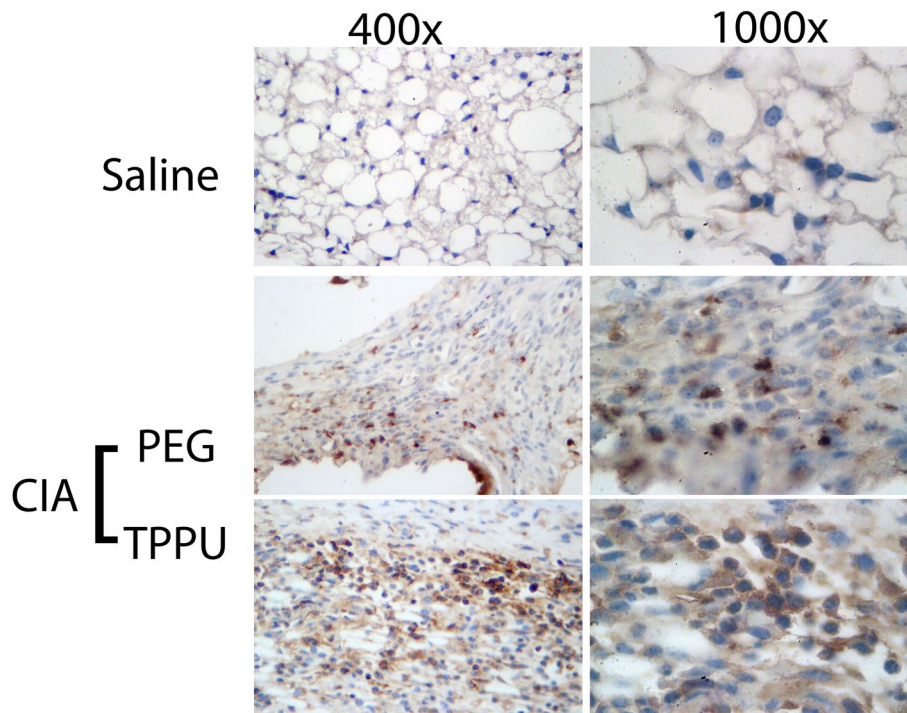


**FIGURE 8** Immunohistochemical staining for FOXP3. Immunostaining was performed in knee joint. Naïve animals showed no immunostaining staining. TPPU-induced exhibited a several positive immunostaining cells and fewer immunostaining cells were observed in the CIA-induced group (400 and 1000 $\times$  magnification)

includes different classes of drugs, which may start with glucocorticoids followed by methotrexate (MTX). Nonetheless, up to 40% of RA patients are resistant to MTX treatment and

this is a consequence of low CD39 expression, a cell surface ectonucleotidases responsible to produce adenosine via ATP degradation. This low expression of CD39 reduces the

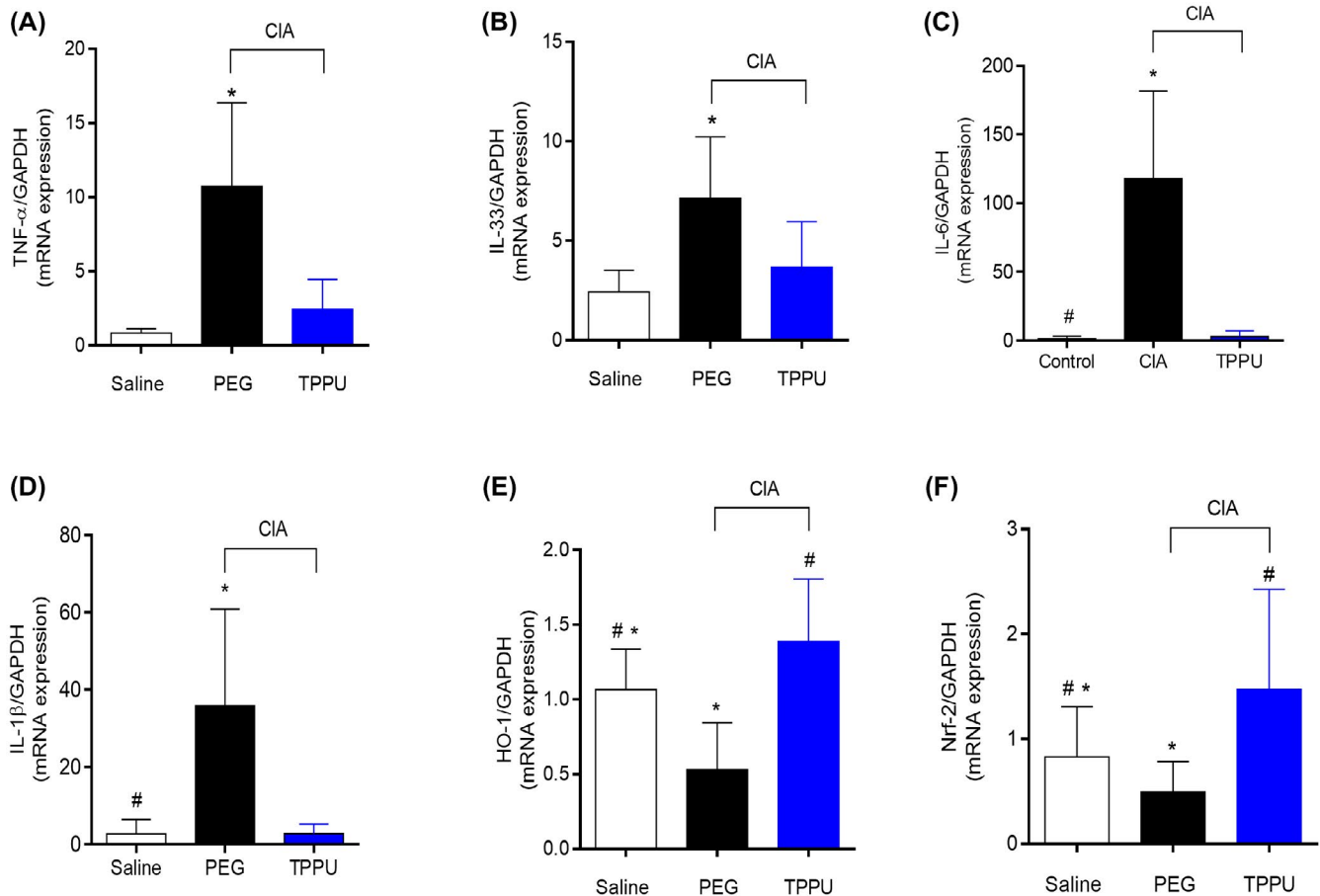


**FIGURE 9** Inhibition of sEH by TPPU induces Heme Oxygenase 1 and decrease expression in pro-inflammatory cytokines on the joints. mRNA quantification to TNF- $\alpha$  (A) IL-33 (B) IL-6 (C) IL-1- $\beta$  (D), HO-1(E) and Nrf2 (F) were performed in joints (soft tissue, fluid and bone) at day 15 of TPPU treatment (n = 6). Expression of soluble Epoxide Hydrolase (sEH) in the joint tissue. # $P$  < .05, significantly different compared with the control (not CIA) group, \* $P$  < .05, significant difference between untreated and TPPU treated CIA groups (one-way ANOVA followed by Tukey test)

suppressive activity of Treg cells via adenosine.<sup>1</sup> In the last 20 years, several Biologic DMARDs were developed although they have diverse side effects,<sup>31</sup> underlying the need for new approaches to treat RA.

In the past few years, sEH inhibitors were shown to be analgesics in neuropathic model and inflammatory models.<sup>17,32</sup> The sEH inhibitor, TPPU (1-trifluoromethoxyphenyl-3-(1-propionylpiperidin-4-yl) urea, has shown efficacy in several animal models, such as inflammatory bone loss,<sup>9,10</sup> LPS-induced pulmonary inflammation,<sup>33</sup> and decreases reperfusion injury after focal cerebral ischemia.<sup>34</sup> In the present study we have demonstrated a potential therapeutic effect of TPPU in RA. This molecule suppresses the inflammatory process due to the promotion of a T regulatory profile, which dampens the Th1 and Th17 cells and alleviates the inflammatory insult into the articular tissue. The animals treated with TPPU showed lower pain, edema and clinical score in comparison to arthritis-induced animals which suggest that TPPU was able to control the severity of the disease. Importantly, it has been demonstrated that oral administration of TPPU

led to systemic distribution as well as high drug levels and thus makes chronic sEH inhibition possible to control inflammatory diseases.<sup>14</sup> Moreover, our results corroborate with a recent study on spontaneous osteoarthritis in old dogs, was able to decrease pain score and increase of mobility function which were observed upon sEH inhibition<sup>11</sup> thus, confirming that sEH inhibition could be a new target and strategy to relieve the pathologic effects of osteoarthritis pain and edema.

sEH expression increases in several diseases,<sup>9,20-22</sup> which in turn decrease several important biological EpFAs. EET are biologically active metabolites of AA, generated by cytochrome p450s (CYP). Once formed, EET are unstable, being rapidly converted into less active or inactive dihydroxyecosatrienoic acids (DHETs) by sEH.<sup>35</sup> Interestingly, it was found that the DHETs generated by sEH were associated with radiographic progression in individuals with osteoarthritis.<sup>36</sup> In the present study, we demonstrated that sEH protein expression levels were increased in CIA animals, which supports a potential contribution of this enzyme in disease. Furthermore, sEH inhibition with TPPU reduced

the disease progression demonstrating an endogenous role of sEH in amplifying the inflammatory response. Interestingly, TPPU also reduced the protein levels of sEH, thus, TPPU not only inhibits the enzymatic activity of sEH, but also the expression of sEH. It is yet unknown the extent that this novel mechanism of TPPU action is relevant in other disease contexts, but it highlights a stronger mechanistic regulation of sEH than previously expected by this enzyme inhibitor, TPPU. In fact, we would expect a possible increase of sEH protein levels as a counteracting mechanism to compensate the inhibition of an enzymatic pathway, yet this increase is not observed. On the other hand, one limitation of the study is the lack of data regarding EET/DHET amount in the analyzed groups.

TPPU showed an anti-inflammatory modulation decreasing TNF- $\alpha$ , interleukin (IL)-1 $\beta$ , and IL-6 levels in a pancreatitis model,<sup>37</sup> but the molecular anti-inflammatory mechanism is not clear in inflammatory models. Toward understanding the molecular mechanism of sEH inhibition in RA, we investigate the effects of TPPU on the polarization of lymphocytes (Th1, Th17 and Treg), a key group of cells in the pathogenesis of RA.<sup>24</sup> The TPPU-treated animals showed decreased expression of several inflammatory genes, including the cytokines IFN- $\gamma$  and IL-12, which have a key role in the Th1 profile.<sup>38</sup> Moreover, Th17 cells are also pivotal therapeutic targets in the context to fight and block autoimmunity disorders like RA. Th17 cells are characterized by transcription factor ROR- $\gamma$ t and produce IL-17, a pro-inflammatory cytokine.<sup>25</sup> Herein, sEH inhibition decreased ROR- $\gamma$ t, IL-23 and IL-17 expression and reduced the profile of polarization to Th17 cells profile (Figure 7). On the other hand, Treg cells are identified by transcription factor Foxp3<sup>26</sup> and have a function of immune regulation and inhibit the development of autoimmune diseases like RA. Cytokines like IL-10 and TGF- $\beta$  are secreted by Treg cells.<sup>39</sup> The inhibition of sEH in CIA mice resulted in an upregulation of Foxp3 and TGF- $\beta$  leading the lymphocytes to a Treg profile. Proinflammatory cytokines such as IL-6 and TNF- $\alpha$  can interfere with the stability of FoxP3 expression in Treg cells, alter the Treg/Teff balance locally or systemically and ultimately provoke a loss of peripheral tolerance.<sup>40</sup> Moreover, DMARDs like Sulfasalazine and leflunomide were cultured with Tregs and both drugs inhibited the anti-proliferative function of Tregs and reduced Treg expression of Foxp3.<sup>41</sup> In the present study, the TPPU treatment was able to decrease IL-1 $\beta$  and IL-6 mRNA expression and increased the expression of FoxP3, stabilizing an immunoregulation by increasing Tregs cells in the joint. However, it is important to note that although TPPU inhibited proinflammatory cytokines and induced the T regulatory cell phenotype, data from previous work using a sepsis model following the use of the sEH inhibitor, markedly improved the survival of septic mice by regulating macrophage functions,

including improved phagocytosis and reduced inflammatory response.<sup>42</sup>

While TPPU increased Foxp3 and TGF- $\beta$  expression, Nrf2, a transcription factor to Heme oxygenase 1 (HO-1) is curiously upregulated in the CIA group treated with TPPU. HO-1 induces an anti-inflammatory response through the regulation of TNF- $\alpha$  levels, and prevents injuries caused by many diseases,<sup>43</sup> especially in arthritis.<sup>44</sup> Recently, TGF- $\beta$  was shown, in culture of human synovial fibroblasts, to stimulate the expression of HO-1.<sup>45</sup> Moreover, NF- $\kappa$ B and Nrf-2 compete for binding sites and the greater expression and activity of Nrf-2 reduces the NF- $\kappa$ B expression.<sup>46</sup> Put together, the data suggest that sEH inhibition reduce RA through the activation of a new anti-inflammatory pathway derived from the activation of Treg cells.

Finally, in the model studied herein, the TPPU treatment was able to decrease IL-33 expression. Interleukin 33 is a pleiotropic cytokine with pronounced pro-inflammatory activity and is involved in the pathogenesis of a variety of diseases. In CIA, the inhibition of IL-33 signaling via its receptor ST2 reduces arthritis severity.<sup>47</sup> IL-33 contributes to the recruitment of neutrophils in RA and the therapeutic anti-TNF therapy mechanism of action depends, at least in part, on reducing ST2 expression by neutrophils diminishing the chemoattraction of RA patients' neutrophils to the joints during the acute inflammatory flares of disease.<sup>48</sup> Furthermore, there is evidence of reciprocal induction of production between TNF $\alpha$  and IL-33,<sup>49,50</sup> which is consistent with our results demonstrating that TPPU reduced the levels of TNF $\alpha$  and IL-33 in CIA.

Taken together, the sEH inhibitor TPPU ameliorates the severity of arthritis by decreasing Th1 and Th17 pathways concomitant with an increase of anti-inflammatory pathways represented by Tregs. Our data also highlight the unexpected downmodulation of sEH levels by TPPU. Thus, TPPU can be used as a new strategy to treat RA and possibly other autoimmune diseases.

## ACKNOWLEDGEMENTS

This work was supported in part by the Brazilian funding agency São Paulo Research Foundation (FAPESP) (#2017/22334-9); Conselho Nacional de Desenvolvimento Científico e Tecnológico (CNPq) - Research Productivity Fellowship to MHN, JTCN, and WAVJ; Programa de Apoio a Grupos de Excelência (PRONEX) grant supported by SETI (Secretaria da Ciência, Tecnologia e Ensino Superior)/Araucária Foundation and MCTIC (Ministério da Ciência, Tecnologia, Inovação e Comunicação)/CNPq; and Paraná State Government (agreement 014/2017, protocol 46.843); Coordenação de Aperfeiçoamento de Pessoal de Nível Superior (CAPES), the National Institute of environmental health and Safety NIEHS R35 ES030443, and NIEHS



Superfund Program P42ES04699 and NIEHS River Award IR35 ES0443-1.


## CONFLICT OF INTEREST

CAT-S, CM and BDH are authors of University of California and synthesis and application of sEHI for disease treatment. BDH is a founder of EiCois LLC which is entering human clinical trial for sEHI.

## AUTHOR CONTRIBUTIONS

J.T. Clemente-Napimoga, B.D. Hammock, and M.H. Napimoga designed research; C.A. Trindade-da-Silva, H.B. Abdalla, S.M. Rosa, C. Ueira-Vieira, and V.A. Martins Montalli, performed research; C.A. Trindade-da-Silva, H.B. Abdalla, S.M. Rosa, C. Ueira-Vieira, C. Morisseau, and W.A. Verri Jr wrote the paper; All authors read and approved the final version of the manuscript.

## ORCID

Carlos A. Trindade-da-Silva  <https://orcid.org/0000-0002-5669-4190>

Juliana T. Clemente-Napimoga  <https://orcid.org/0000-0003-1068-3039>

Henrique B. Abdalla  <https://orcid.org/0000-0002-7517-2830>

Sergio Marcolino Rosa  <https://orcid.org/0000-0002-8501-4721>


Carlos Ueira-Vieira  <https://orcid.org/0000-0002-8369-9069>

Christophe Morisseau  <https://orcid.org/0000-0002-5672-6631>

Waldiceu A. Verri  <https://orcid.org/0000-0003-2756-9283>

Victor Angelo Martins Montalli  <https://orcid.org/0000-0002-1927-7718>

Bruce D. Hammock  <https://orcid.org/0000-0003-1408-8317>

Marcelo H. Napimoga  <https://orcid.org/0000-0003-4472-365X>

## REFERENCES

- Xu D, Jiang HR, Kewin P, et al. IL-33 exacerbates antigen induced arthritis by activating mast cells. *Proc Natl Acad Sci U S A*. 2008;105:10913-10918.
- Chatzidionysiou K, Emamikia S, Nam J, et al. Efficacy of glucocorticoids, conventional and targeted synthetic disease-modifying antirheumatic drugs: a systematic literature review informing the 2016 update of the EULAR recommendations for the management of rheumatoid arthritis. *Ann Rheum Dis*. 2017;76:1102-1107.
- Peres RS, Liew FY, Talbot J, et al. Low expression of CD39 on regulatory T cells as a biomarker for resistance to methotrexate therapy in rheumatoid arthritis. *Proc Natl Acad Sci U S A*. 2015;112:2509-2514.
- Dinarello CA. Anti-cytokine therapeutics and infections. *Vaccine*. 2003;21:S24-S34.
- Sultana S, Bishayi B. Neutralization of TNFR-1 and TNFR-2 modulates *S aureus* induced septic arthritis by regulating the levels of pro inflammatory and anti-inflammatory cytokines during the progression of the disease. *Immunol Lett*. 2018;196:33-51.
- Kodani SD, Morisseau C. Role of epoxy-fatty acids and epoxide hydrolases in the pathology of neuro-inflammation. *Biochimie*. 2019;159:59-65.
- Harris TR, Hammock BD. Soluble epoxide hydrolase: gene structure, expression and deletion. *Gene*. 2013;526:61-74.
- Rose TE, Morisseau C, Liu JY, et al. 1-Aryl-3-(1-acylpiperidin-4-yl)urea inhibitors of human and murine soluble epoxide hydrolase: structure-activity relationships, pharmacokinetics, and reduction of inflammatory pain. *J Med Chem*. 2010;14:7067-7075.
- Trindade-da-Silva CA, Bettaieb A, Napimoga MH, et al. Soluble epoxide hydrolase pharmacological inhibition decreases alveolar bone loss by modulating host inflammatory response, RANK-related signaling, endoplasmic reticulum stress, and apoptosis. *J Pharmacol Exp Ther*. 2017;361:408-416.
- Napimoga MH, Rocha EP, Trindade-da-Silva CA, et al. Soluble epoxide hydrolase inhibitor promotes immunomodulation to inhibit bone resorption. *J Periodontol Res*. 2018;53:743-749.
- McReynolds CB, Hwang SH, Yang J, et al. Pharmaceutical effects of inhibiting the soluble epoxide hydrolase in canine osteoarthritis. *Front Pharmacol*. 2019;31(10):533. <https://doi.org/10.3389/fphar.2019.00533>
- Sakaguchi S, Wing K, Onishi Y, Prieto-Martin P, Yamaguchi T. Regulatory T cells: how do they suppress immune responses? *Int Immunol*. 2009;21:1105-1111.
- Carregaro V, Napimoga MH, Peres RS, et al. Therapeutic treatment of arthritic mice with 15-deoxy  $\Delta^{12,14}$ -prostaglandin J2 (15d-PGJ2) ameliorates disease through the suppression of Th17 cells and the induction of CD4+CD25-FOXP3+ cells. *Mediators Inflamm*. 2016;2016:9626427.
- Osterman C, McCarthy MB, Cote MP, et al. Platelet-rich plasma increases anti-inflammatory markers in a human coculture model for osteoarthritis. *Am J Sports Med*. 2015;43:1474-1484.
- Su Z, Shotorbani SS, Jiang X, et al. A method of experimental rheumatoid arthritis induction using collagen type II isolated from chicken sternal cartilage. *Mol Med Rep*. 2013;8:113-117.
- Carregaro V, Sá-Nunes A, Cunha TM, et al. Nucleosides from phlebotomus papatasi salivary gland ameliorate murine collagen-induced arthritis by impairing dendritic cell functions. *J Immunol*. 2011;187:4347-4359.
- Inceoglu B, Wagner KM, Yang J, et al. Acute augmentation of epoxygenated fatty acid levels rapidly reduces pain-related behavior in a rat model of type I diabetes. *Proc Natl Acad Sci U S A*. 2012;109:11390-11395.
- Borghi SM, Mizokami SS, Pinho-Ribeiro FA, et al. The flavonoid quercetin inhibits titanium dioxide (TiO<sub>2</sub>)-induced chronic arthritis in mice. *J Nutr Biochem*. 2018;53:81-95.
- Ruiz-Miyazawa KW, Staurengo-Ferrari L, Pinho-Ribeiro FA, et al. 15d-PGJ2-loaded nanocapsules ameliorate experimental gout arthritis by reducing pain and inflammation in a PPAR-gamma-sensitive manner in mice. *Sci Rep*. 2018;18:13979.
- Faulkner J, Pye C, Al-Shabrawey M, Elmarakby AA. Inhibition of 12/15-lipoxygenase reduces renal inflammation and injury in streptozotocin-induced diabetic mice. *J Diabetes Metab*. 2015;6:555.

21. Yao L, Cao B, Cheng Q, et al. Inhibition of soluble epoxide hydrolase ameliorates hyperhomocysteinemia-induced hepatic steatosis by enhancing  $\beta$ -oxidation of fatty acid in mice. *Am J Physiol Gastrointest Liver Physiol*. 2019;316:G527-G538.
22. Park B, Corson TW. Soluble epoxide hydrolase inhibition for ocular diseases: vision for the future. *Front Pharmacol*. 2019;7:10-95.
23. Tsai HJ, Hwang SH, Morisseau C, et al. Pharmacokinetic screening of soluble epoxide hydrolase inhibitors in dogs. *Eur J Pharm Sci*. 2010;40:222-238.
24. Kamali AN, Noorbakhsh SM, Hamedifar H, et al. A role for Th1-like Th17 cells in the pathogenesis of inflammatory and autoimmune disorders. *Mol Immunol*. 2019;105:107-115.
25. Huh JR, Littman DR. Small molecule inhibitors of ROR $\gamma$ t: targeting Th17 cells and other applications. *Eur J Immunol*. 2012;42:2232-2237.
26. Yu Q, Xu M, Yu F, Jin Y. CD4(+)CD25(+) regulatory T cells as a therapeutic target in rheumatoid arthritis. *Cent Eur J Immunol*. 2014;39:100-103.
27. Loboda A, Damulewicz M, Pyza E, Jozkowicz A, Dulak J. Role of Nrf2/HO-1 system in development, oxidative stress response and diseases: an evolutionarily conserved mechanism. *Cell Mol Life Sci*. 2016;73:3221-3247.
28. Park J, Mendy A, Vieira ER. Various types of arthritis in the United States: prevalence and age-related trends from 1999 to 2014. *Am J Public Health*. 2018;108:256-258.
29. Otter SJ, Lucas K, Springett K, et al. Foot pain in rheumatoid arthritis prevalence, risk factors and management: an epidemiological study. *Clin Rheumatol*. 2010;29:255-271.
30. Firestein GS, McInnes IB. Immunopathogenesis of rheumatoid arthritis. *Immunity*. 2017;46:183-196.
31. Köhler BM, Günther J, Kaudewitz D, Lorenz HM. Current therapeutic options in the treatment of rheumatoid arthritis. *J Clin Med*. 2019;28:938. <https://doi.org/10.3390/jcm8070938>
32. Inceoglu B, Bettaieb A, Trindade da Silva CA, Lee KS, Haj FG, Hammock BD. Endoplasmic reticulum stress in the peripheral nervous system is a significant driver of neuropathic pain. *Proc Natl Acad Sci U S A*. 2015;112:9082-9087.
33. Dong R, Hu D, Yang Y, et al. EET reduces LPS-induced hyperpermeability by targeting GRP78 mediated Src activation and subsequent Rho/ROCK signaling pathway. *Oncotarget*. 2017;8:50958-50971.
34. Tu R, Armstrong J, Lee KSS, Hammock BD, Sapirstein A, Koehler RC. Soluble epoxide hydrolase inhibition decreases reperfusion injury after focal cerebral ischemia. *Sci Rep*. 2018;8:5279.
35. Wagner KM, McReynolds CB, Schmidt WK, Hammock BD. Soluble epoxide hydrolase as a therapeutic target for pain, inflammatory and neurodegenerative diseases. *Pharmacol Ther*. 2017;180:62-76.
36. Valdes AM, Ravipati S, Pousinis P, et al. Omega-6 oxylipins generated by soluble epoxide hydrolase are associated with knee osteoarthritis. *J Lipid Res*. 2018;59:1763-1770.
37. Bettaieb A, Chahed S, Bachaalany S, Griffey S, Hammock BD, Haj FG. Soluble epoxide hydrolase pharmacological inhibition ameliorates experimental acute pancreatitis in mice. *Mol Pharmacol*. 2015;88:281-290.
38. Oestreich KJ, Weinmann AS. T-bet employs diverse regulatory mechanisms to repress transcription. *Trends Immunol*. 2012;33:78-83.
39. Nie H, Zheng Y, Li R, et al. Phosphorylation of Foxp3 controls regulatory T cell function and is inhibited by TNF- $\alpha$  in rheumatoid arthritis. *Nat Med*. 2013;19:322-328.
40. Attias M, Al-Aubodah T, Piccirillo CA. Mechanisms of human FoxP3(+) T(reg) cell development and function in health and disease. *Clin Exp Immunol*. 2019;197:36-51.
41. Oh JS, Kim YG, Lee SG, et al. The effect of various disease-modifying anti-rheumatic drugs on the suppressive function of CD4+CD25+ regulatory T cells. *Rheumatol Int*. 2013;33:381-388.
42. Chen Z, Tang Y, Yu J, et al. sEH Inhibitor TPPU ameliorates cecal ligation and puncture-induced sepsis by regulating macrophage functions. *Shock*. 2019. <https://doi.org/10.1097/SHK.0000000000001408>
43. Yin H, Li X, Yuan B, et al. Heme oxygenase-1 ameliorates LPS-induced acute lung injury correlated with downregulation of interleukin-33. *Int Immunopharmacol*. 2011;11:2112-2117.
44. Kobayashi H, Takeno M, Saito T, et al. Regulatory role of heme oxygenase 1 in inflammation of rheumatoid arthritis. *Arthritis Rheum*. 2006;54:1132-1142.
45. Kuo SJ, Yang WH, Liu SC, Tsai CH, Hsu HC, Tang CH. Transforming growth factor  $\beta$ 1 enhances heme oxygenase 1 expression in human synovial fibroblasts by inhibiting microRNA 519b synthesis. *PLoS ONE*. 2017;12:e0176052.
46. Staurengo-Ferrari L, Badaro-Garcia S, Hohmann MSN, et al. Contribution of Nrf2 modulation to the mechanism of action of analgesic and anti-inflammatory drugs in pre-clinical and clinical stages. *Front Pharmacol*. 2019;11:1536.
47. Xu D, Jiang HR, Li Y, et al. IL-33 exacerbates autoantibody-induced arthritis. *J Immunol*. 2010;184:2620-2626.
48. Verri WA, Souto FO, Vieira SM, et al. IL-33 induces neutrophil migration in rheumatoid arthritis and is a target of anti-TNF therapy. *Ann Rheum Dis*. 2010;69:1697-1703.
49. Zarpelon AC, Cunha TM, Alves-Filho JC, et al. IL-33/ST2 signaling contributes to carrageenin-induced innate inflammation and inflammatory pain: role of cytokines, endothelin-1 and prostaglandin E2. *Br J Pharmacol*. 2013;169:90-101.
50. Zarpelon AC, Rodrigues FC, Lopes AH, et al. Spinal cord oligodendrocyte-derived alarmin IL-33 mediates neuropathic pain. *FASEB J*. 2016;30:54-65.

## SUPPORTING INFORMATION

Additional Supporting Information may be found online in the Supporting Information section.

**How to cite this article:** Trindade-da-Silva CA, Clemente-Napimoga JT, Abdalla HB, et al. Soluble epoxide hydrolase inhibitor, TPPU, increases regulatory T cells pathway in an arthritis model. *The FASEB Journal*. 2020;34:9074–9086. <https://doi.org/10.1096/fj.202000415R>